

EvoPhylo: an R package for pre- and postprocessing of morphological data from relaxed clock Bayesian phylogenetics

Tiago R. Simões^{1,*}, Noah Greifer², Joëlle Barido-Sottani³ and Stephanie E. Pierce¹

¹*Museum of Comparative Zoology & Department of Organismic and Evolutionary Biology,
Harvard University, Cambridge, MA 02138, USA.*

²*Institute for Quantitative Social Science, Harvard University, Cambridge, MA 02138, USA.*

³*Institut de Biologie de l'ENS (IBENS), École normale supérieure, CNRS, INSERM, Université
PSL, 75005 Paris, France.*

*Corresponding Author: tsimoes@fas.harvard.edu

Abstract

1. Relaxed clock Bayesian evolutionary inference (BEI) enables the co-estimation of phylogenetic trees and evolutionary parameters associated with models of character and lineage evolution. Fast advances in new model developments over the past decade have boosted BEI as a major macroevolutionary analytical framework using morphological and/or molecular data across vastly different study systems. However, there is a limited availability of bioinformatic tools to pre- and post-process data from BEI, such as identifying morphological data partitions, or statistically testing and creating publication quality plots of evolutionary hypotheses using the output from BEI.

2. Here we introduce *EvoPhylo*, an R package to perform automated morphological character partitioning for phylogenetic analyses and analyze macroevolutionary parameter outputs from relaxed clock (time-calibrated) BEI.

3. We present the theoretical background behind *EvoPhylo*'s functions and analytical tools for evolutionary hypothesis testing, its potential uses, and interpretation of its results with a series of vignettes and links to a step-by-step tutorial.

4. *EvoPhylo* will facilitate utilization of Bayesian relaxed clocks as a tool for macroevolutionary inference across a wide range of users and fields of research, especially those that use morphological datasets.

Keywords: Bayesian phylogenetics, character partitioning, evolutionary rates, selection, diversification rates, morphology, R.

35 1. INTRODUCTION

36 Macroevolutionary research programs have historically relied upon the utilization of a
37 given phylogenetic tree (or set of trees) to subsequently estimate the tempo and mode (rates and
38 model) of morphological, ecological, and molecular traits (Morlon, 2014; Pennell & Harmon,
39 2013). These techniques, known collectively as phylogenetic comparative methods (Felsenstein,
40 1985), have revolutionized quantitative approaches to infer processes and patterns of evolution for
41 a wide spectrum of living and fossil organisms across vastly different scales of time (Morlon, 2014;
42 Pennell & Harmon, 2013; Slater & Harmon, 2013). In such approaches, evolutionary parameter
43 estimates are obtained *a posteriori* from phylogenetic inference, and the structure of the
44 phylogenetic tree (tree topology) and its branch lengths (as accumulated substitutions or as units
45 of time) are used as input for downstream analyses and are necessarily treated as a fixed parameter.
46 However, the true topology and branch lengths of phylogenetic trees are never known with
47 certainty. Additionally, just as phylogenetic trees are necessary to estimate the tempo and mode of
48 lineage and character evolution, understanding the tempo and mode of character and lineage
49 evolution are also necessary to infer phylogenetic trees to begin with.

50 Bayesian evolutionary inference (BEI) using relaxed clocks circumvent such conundrums
51 by jointly estimating tree topology and branch lengths along with evolutionary parameters,
52 including divergence times, evolutionary rates, and rates of lineage diversification, using
53 molecular data, morphological data, or both (Drummond et al., 2006; Gavryushkina et al., 2017;
54 Höhna et al., 2016; Lee et al., 2014; A. Wright et al., 2020). However, until recently it was not
55 feasible to conduct such analyses beyond relatively small datasets due to: 1) the high
56 computational burden of estimating joint posterior probabilities of dozens of parameters; 2) the
57 limited availability of tree and clock models concomitant with a limited understanding of the
58 performance; and 3) limited bioinformatics tools to assess evolutionary parameters output by such
59 analyses. Fortunately, the last decade was marked by increased academic access to high
60 performance computing facilities, including the CIPRES Gateway (Miller et al., 2012).
61 Additionally, there have been major advances on tree modeling, such as the fossilized birth-death
62 (FBD) tree model and its skyline variant (SFBD), which allow speciation, extinction and
63 fossilization parameters to vary across time bins (Gavryushkina et al., 2014; Heath et al., 2014;
64 Stadler, 2010, 2011; Zhang et al., 2016). More recently, performance studies revealed that these
65 models can provide accurate estimates of macroevolutionary parameters, including net
66 diversification, turnover, and fossil sampling rates (Luo et al., 2020; Warnock et al., 2020).
67 Relaxed clocks can also provide reliable rate estimates even with highly limited taxonomic
68 sampling (Ho et al., 2005), and a variety of new clock models have been proposed (Bielejec et al.,
69 2014; Fourment & Darling, 2018; Zhang, 2021). As a result of these advances, there has been a
70 recent boost in macroevolution studies using BEI to infer evolutionary parameters for various
71 modern and extinct lineages representing datasets of various compositions and sizes (King et al.,
72 2017; Lee et al., 2013, 2014; Simões, Vernygora, et al., 2020; Simões & Pierce, 2021; A. Wright
73 et al., 2020).

74 Bioinformatics tools to explore the rich amount of data output from BEI have also been
75 thoroughly expanded. Such tools include software and packages to analyze the posterior trace files
76 between multiple runs or MCMC chains, such as the standalone program Tracer (Rambaut et al.,
77 2018) and the R package *RWTY* (Warren et al., 2017), or to visualize and plot divergence times
78 and rates of evolution parameters on trees, including FigTree (Rambaut, 2018), DensiTree (R. R.
79 Bouckaert, 2010), the R package *ggtree* (Yu et al., 2017). However, there are few tools currently
80 available to extract, plot, summarize statistically, and conduct further downstream analyses from
81 evolutionary parameters obtained from relaxed clock BEI. These include statistically testing the
82 difference of evolution rates between clock partitions and/or evolutionary lineages, how such
83 differences impact our understanding of the mode of selection upon those lineages, or the rate of
84 diversification dynamics across time—but see RevGadgets (Tribble et al., 2022) for a recent
85 implementation of the latter for outputs from the software package RevBayes (Höhna et al., 2016).
86 Additionally, differently from molecular data—e.g., (Duchêne et al., 2014; Lanfear et al., 2016)—
87 there are limited attempts to pre-process morphological datasets to detect data partitions that
88 should be analyzed using independent evolutionary clock models for BEI.

89 Here we introduce *EvoPhylo*, an R package to perform pre- and post-processing of the
90 input and output from BEI. It includes automated partitioning of phenotypic (i.e., morphological)
91 character data for BEI, and statistical tools to plot and analyze macroevolutionary parameter
92 outputs from clock (time-calibrated) BEI analyses. In this paper, we present the theoretical
93 background behind *EvoPhylo* and describe its potential uses, overall functionality, and the
94 interpretation of its results through demonstration with real datasets and links to online vignettes
95 with step-by-step tutorials.

96

97 **2. CHARACTER PARTITIONING**

98 **2.1 Clustering method**

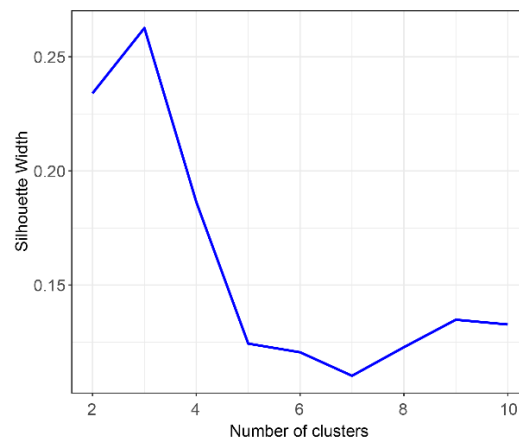
99 A common approach to data partitioning (i.e., clustering) is the extraction of Euclidean distances
100 between data points, from which a distance matrix “D” is calculated, and subsequently used to
101 detect data partitions (clusters) using K-means, or ordination approaches such as principal
102 coordinate analysis (PCoA). Indeed, the first attempts to automatically partition morphological
103 characters have explored these approaches (Goswami & Polly, 2010; Lanfear et al., 2016).
104 However, recent studies have indicated that Euclidean distances can be extremely sensitive to
105 missing data, and alternative choices such as Gower distances (Gower, 1971) provide more
106 suitable alternatives for the handling of missing data (Lehmann et al., 2019; Lloyd, 2016). This
107 issue creates a subsequent problem for estimating clusters using K-means, as the latter depends on
108 a Euclidean-based distance matrix. Further, K-means are based on measuring the distance between
109 samples and cluster centroids (i.e., the center of mass or mean vector of the cluster). The mean
110 vector is particularly sensitive to outliers (as any other mean estimate) (Rencher & Christensen,
111 2012), making its use especially problematic for small-sized clusters or clusters of drastically
112 different sizes, which are to be expected from most standard sized morphological datasets.

113 *EvoPhylo* uses Gower distances to create the inter-character distance matrix “D” and
114 conducts a clustering analysis of morphological data with partitioning around medoids (PAM, also
115 known as K-medoids), which can estimate clusters (i.e., partitions) using Gower distances,
116 following its first implementation by Simões & Pierce (2021). PAM is analogous to K-means, but
117 the resulting clusters are centered around medoids instead of around centroids, making them less
118 sensitive to outliers and heterogeneous cluster sizes (Budiaji & Leisch, 2019; Rencher &
119 Christensen, 2012).

120 To define how many clusters the data could be partitioned into, various PAM partitioning
121 schemes are tested and the quality of each clustering scheme is determined using the silhouette
122 index (Si) approach (Rousseeuw, 1987), a method that estimates how well an object falls within
123 its cluster compared to other clusters (Fig. 1). The PAM partitioning schemes to be tested should
124 range from K=2 to a large number of partitions (user-defined, default K = 10). The best partitioning
125 scheme from PAM+Si can be exported into a Nexus file with the *cluster_to_nexus* function,
126 including the list of characters and their respective partitions (Fig. 2). The contents can be copied
127 and pasted directly into a Mr. Bayes commands block for a partitioned clock Bayesian inference
128 analysis.

129

```
### 1. Generate distance matrix  
#Load data matrix and  
#produce a Gower distance matrix  
d_matrix <- get_gower_dist(  
  "DataMatrix.nex",  
  numeric = FALSE)  
  
### 2. Estimate optimal number of partitions  
sw <- get_sil_widths(  
  dist_matrix,  
  max.k = 10)  
plot(sw, color = "blue", size = 1)
```



130
131 **Fig. 1.** Silhouette index plot indicating the higher quality of clustering when the number of
132 partitions (k) = 3.
133

134 2.2 Selecting best candidate partitioning scheme

135 For further (and independent) testing of the quality of the chosen partitioning scheme, we also
136 provide a graphic visualization approach based on a Barnes-Hut t-Distributed Stochastic Neighbor
137 Embedding (t-SNE) (Van Der Maaten & Hinton, 2008). More traditional ordination procedures,
138 such as principal components analysis (PCA, for continuous data) or PCoA (for discrete data), can
139 preserve the linear relationship between data points at a lower dimensionality. However, because
140 those procedures try to preserve the local distances between data points, they become less efficient
141 at characterizing the overall structure of high dimensional data. Here, it is more important to reduce
142 the local linear distance between similar (neighboring) data points while maximizing the distance

143 between distant datapoints (Van Der Maaten & Hinton, 2008); for such cases, nonlinear ordination
 144 procedures are preferred for observing the overall data structure in a reduced number of
 145 dimensions. t-SNE has been demonstrated to be more efficient at preserving both local and global
 146 structures when reducing high dimensional data into only two or three dimensions compared to
 147 other nonlinear ordination procedures (Van Der Maaten, 2009), thus offering an important
 148 advantage over previously utilized graphic approaches to determine morphological clusters such
 149 as PCoA.

150 *EvoPhylo* combines PAM+Si clustering with t-SNE within the function *make_clusters*, by
 151 allowing the user to request displaying the distance between data points and in ordination space
 152 through the argument *tsne=TRUE*. Users can choose the representation of two or more dimensions
 153 and also the variable theta, which controls the speed/trade off accuracy of t-SNE calculations,
 154 through the *tsne_dim* and *tsne_theta* arguments, respectively.

155 *EvoPhylo* automatically colors individual data points in the t-SNE plots according to the
 156 partitioning scheme identified with PAM+Si, allowing users to quickly verify if both strategies
 157 converge on the number and composition of each character partition. This is the case with the
 158 example dataset used here from Simões & Pierce (2021) (Fig. 2). If there is a mismatch between
 159 the partitioning scheme from PAM+Si and that displayed in the t-SNE plots, we recommend re-
 160 plotting t-SNEs using another coloring scheme for the data points, such as one based on
 161 anatomically defined character partitions. The latter can be accomplished by directly utilizing
 162 arguments within the *Rtsne* function of the *Rtsne* package (Krijthe, 2015). If there is a closer
 163 correspondence between tSNEs and anatomical partitioning as compared to PAM+Si and tSNEs,
 164 it is reasonable to follow anatomical partitioning.

165
166

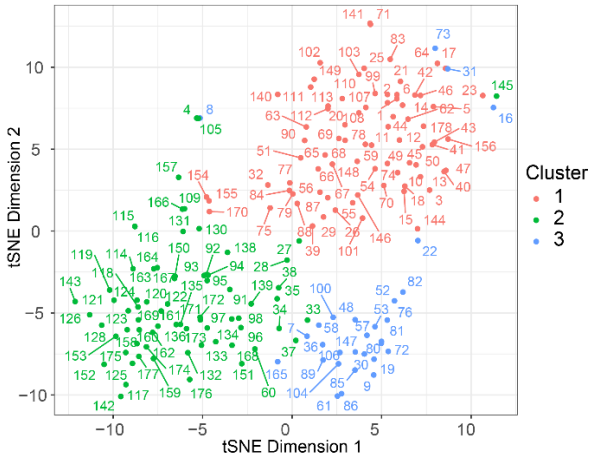
```

### 3. Calculate partitions (clusters)
#PAM+Si (plotted using t-SNE)
clusters <- make_clusters(
  dist_matrix,
  k = 3, tsne = TRUE,
  tsne_dim = 2)

plot(clusters, nrow = 1,
     max.overlaps = 12)

#Write partitions to Nexus file
cluster_to_nexus(clusters,
  file = "Clusters_Nexus.txt")

```



167
168 **Fig. 2.** Plot of identified morphological partitions using tSNE of the first two dimensions with
 169 data points colored according to the partitioning scheme determined by PAM+Si.
 170

171 2.3 Data treatment and import

172 Categorical data (such as discrete morphological characters) should be treated as factors
173 when imported to calculate character distances, as the symbols used to represent different character
174 states are arbitrary (e.g., could be equally represented by letters, such as for DNA data). If
175 continuous variables are used as phylogenetic characters, those should be read in from a separate
176 file and treated as numeric data, since input values for each state (e.g., 0.234; 2.456; 3.567; etc.)
177 represent true distances between data points.

178 Additionally, most morphological datasets have a portion of inapplicable or missing
179 characters, which introduce problems to calculate distance matrices. Inapplicable and missing data
180 (typically scored as “-” and “?”, respectively) are interpreted as extra states relative to numerical
181 symbols typically used for different character states (“0”, “1”, “2”, etc.). Therefore, there are a few
182 options users may follow for handling morphological phylogenetic datasets to account for
183 inapplicable/missing data before importing it into *EvoPhylo*. Users may either convert
184 inapplicable/missing to “NA” or they may choose to keep the original symbols.

185 As demonstrated by the example provided in the [online vignette](#), converting
186 inapplicable/missing conditions to “NA” introduces “NaN” scores to every pairwise comparison
187 involving two characters with “NA” when calculating a distance matrix. Statistical tests and
188 clustering methods cannot utilize such matrices with “NaN” as data entries, and so the removal of
189 observations contributing to excessive NaN would have to be performed—such as done by the
190 package *Claddis* (Lloyd, 2016) when calculating an inter-taxon distance matrices to estimate
191 morphospace. However, removing observations with excessive inapplicable/missing data is not
192 possible for character partitioning because each character in the dataset must be assigned to at least
193 one partition (regardless of the amount of missing or inapplicable data). Furthermore, comparisons
194 between any characters in which one character has an “NA” score will result in a distance of 0
195 between these same characters (Table 2 in the [online vignette](#)). Therefore, the implicit assumption
196 with this strategy is that unknown characters contribute 0 distance (i.e., unknown states are
197 assumed to be equal to the known states), which biases the distance matrix by minimizing the
198 overall distance between characters to the lowest possible values.

199 Alternatively, users may keep the original inapplicable/missing data (although all must be
200 represented by the same symbol, e.g., all as “?”), and such states will be treated as a distinct
201 categorical variable relative to numeric symbols. As a result, pairwise comparisons with characters
202 with unknown states avoid the introduction of ‘NaN’ in the distance matrix. This approach
203 assumes that unknown states are always different from any known states, which will bias the
204 distance matrix by increasing the overall distance between characters. Fortunately, however,
205 Gower distances (as used here) are normalized by the number of variables in the dataset (number
206 of taxa in this case) (Gower, 1971), which reduces this bias. For instance, in a simple comparison
207 between two characters sampled from two taxa (A and B), e.g., character 6 (1,1) and character 7
208 (NA, 1) from the example in the [online vignette](#), the raw distance between these characters is 1.0,
209 but the Gower distance between them is $1/2 = 0.5$. Therefore, we recommend this approach to

210 calculate inter-character distance matrices, which only requires users to convert all
211 inapplicable/missing scores in their datasets to “?” symbols before importing into *EvoPhylo*.

212 We note, however, that there is no objective solution to the problem of inapplicable/missing
213 data to estimate distance matrices, besides potentially negatively impacting the accuracy of
214 phylogenetic analyses—e.g., (Vernygora et al., 2020; A. M. Wright & Hillis, 2014), but see
215 Keating (2020). We thus suggest avoiding or removing such characters from morphological
216 phylogenetic datasets whenever possible as a general good practice.

217

218 3. CLOCK RATES AND SELECTION MODE

219 With the assumption that morphological evolution is mostly driven by adaptive change, it
220 is possible to infer the mode of natural selection operating upon particular regions of the phenotype
221 (e.g., morphological or morphological partitions) and across distinct clades in a phylogeny as a
222 function of their morphological evolutionary rates (Baker et al., 2016; Revell et al., 2012; Simões
223 & Pierce, 2021; Venditti et al., 2011). Evolutionary rates that are significantly accelerated relative
224 to the background rates provide support for positive or directional morphological selection in
225 analogy with the d_N/d_S ratio in molecular evolution, whereas strongly decelerating rates indicate
226 stabilizing selection, stasis or constraint (Baker et al., 2016; Yang, 2014). This concept was first
227 applied to morphological traits using continuous data in phylogenetic comparative methods in the
228 program BayesTraits (Baker et al., 2016) and later extended to discrete data and evolutionary rates
229 estimated with Bayesian molecular or morphological clocks (Simões & Pierce, 2021), and it is the
230 basis for inferring the strength and mode of selection in *EvoPhylo*.

231 The original approach in BayesTraits takes the clock rate on every tree branch (Δv), which
232 is then compared to the background rate of evolution (Δb), forming the rate scalar ratio ($r = \Delta v$
233 $/\Delta b$), as defined by Baker et al., (2016). This measure is equivalent to the interpretation of relative
234 rates of character evolution produced by relaxed Bayesian clocks, in which estimates greater than
235 1 indicate rates above background rate levels (the base of the clock rate) and are therefore
236 accelerating, whereas relative branch rate values less than 1 indicate values below background rate
237 levels, implying a decrease in the rates of evolution in that branch (Ronquist et al., 2019).

238 To draw evolution rates from Bayesian trees and infer selection mode, users must first use
239 the function `get_clockrate_table` to extract relative clock rate values from every branch of a relaxed
240 clock Bayesian inference tree—i.e., median or mean rate values embedded in summary tree files
241 produced by relaxed clock Bayesian inference. An argument `drop_dummyextant` is available to
242 allow users to automatically remove a “dummy” extant taxon introduced for the offsetting of all
243 tree node ages when analyzing fossil-only datasets that incorporate uncertainty in the age of every
244 tip age—see discussions in Simões & Pierce (2021) for further details.

```

### 1. Import summary tree
tree<-treeio::read.mrbayes(
  "MultiClockTree/Tree_3p.t")

### 2. Get and export rate tables
RateTable_Medians_no_clades <-
  get_clockrate_table
  (tree, summary = "median")

write.csv(RateTable_Medians_no_clades,
  file="RateTable_Medians.csv")

### 3. Import rate table
#with custom clade memberships added
RateTable_Medians<- read.csv(
  "RateTable_Medians_Clades.csv",
  header = TRUE)

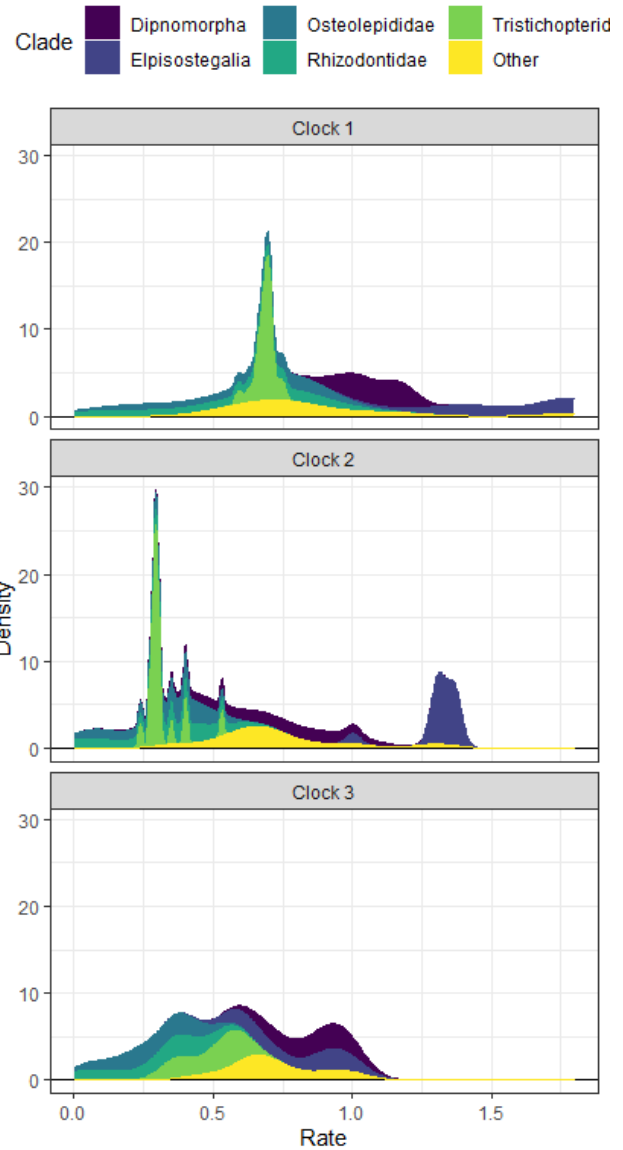
### 4. Get summary stats
#for each clade/clock partition
clockrate_summary(RateTable_Medians,
  "Sum_RateTable_Medians_Clades.csv",
  digits=2)

### 5. Plot rates by clock partition/clade
# with stacked plots (viridis)
clockrate_dens_plot(RateTable_Medians,
  stack = TRUE, nrow = 3,
  scales = "fixed")+
  ggplot2::scale_color_viridis_d() +
  ggplot2::scale_fill_viridis_d()

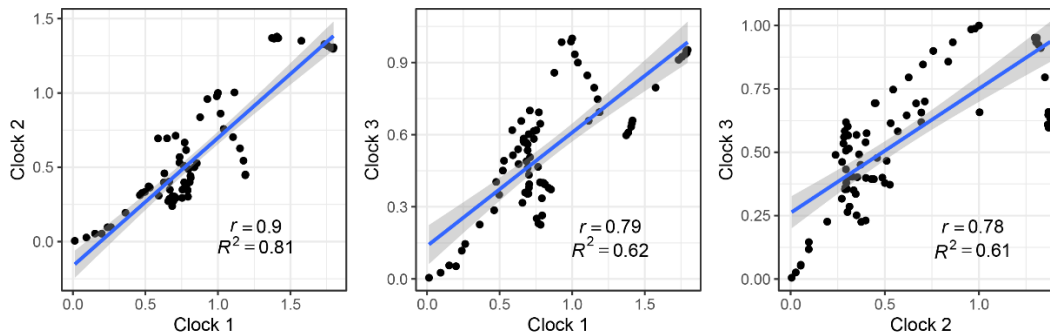
### 7. Get rate Linear models
p1<- clockrate_reg_plot(RateTable_Medians,
  clock_x = 1, clock_y = 2)
p2<- clockrate_reg_plot(RateTable_Medians,
  clock_x = 1, clock_y = 3)
p3<- clockrate_reg_plot(RateTable_Medians,
  clock_x = 2, clock_y = 3)

p1 + p2 + p3 + plot_layout(nrow = 1)

```



245
246



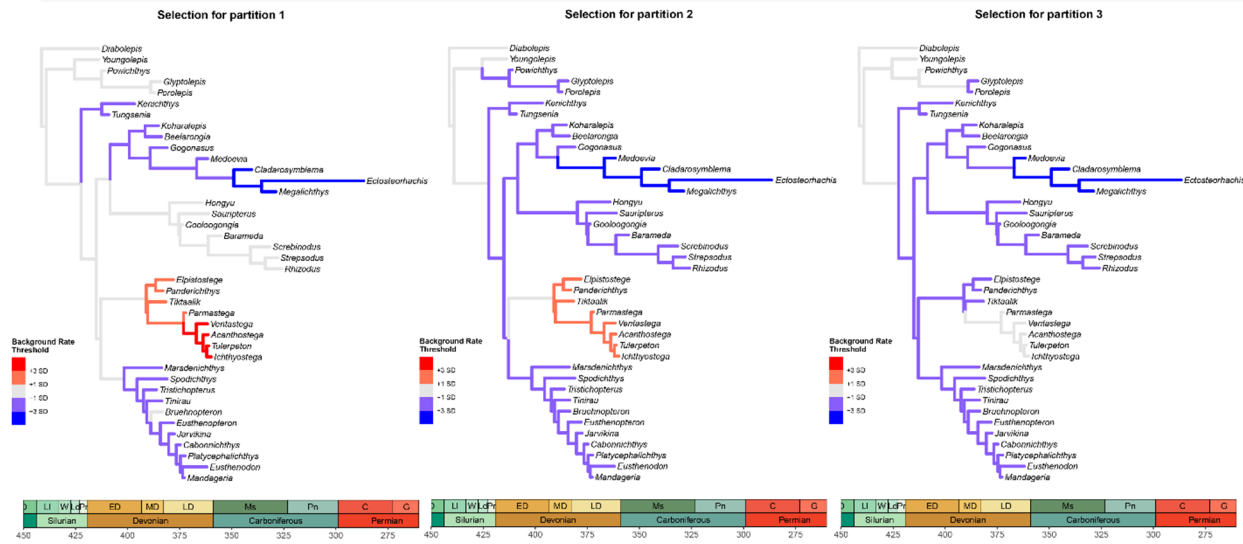
247
248
249
250

Fig. 3. Summary statistics and plots for clock (evolutionary) rates by clade and clock partitions.

251 At this stage, rate tables must have customizable clade names (specific for each dataset and
 252 tree topology). This can be done within R or by exporting rates tables to a CSV file (and edited in,
 253 e.g., Microsoft Excel) and manually adding a "clade" column using the tree node numbers as
 254 reference; a sample dataset of this kind is provided with *EvoPhylo* and can be called with
 255 *rate_table_clades_means*. The new rates tables with added clade names must then be used for
 256 downstream analyses. Detailed examples are provided in the [online vignette](#).

```

 257
 258 ### 1. Import and transform mean rate table with custom clade memberships
 259 RateTable_Means<- read.csv("RateTable_Means_Clades.csv", header = TRUE)
 260 RatesByClade <- clock_reshape(RateTable_Means)
 261
 262 ### 2. Import all log (.p) files from all runs and combine them
 263 Comb_posterior3p <- combine_log("LogFiles3p", burnin = 0.25, downsample = 2500)
 264
 265 ### 3. Pairwise t-tests of Rate values
 266 RateSign_tests<- get_pwt_rates(RateTable_Means, Comb_posterior3p)
 267
 268 ### 4. Plot selection strength on the summary tree using thresholds for each clock partition
 269 S1<-plot_treerates_sgn(tree, Comb_posterior3p,
 270   clock = 1,           #Show rates for clock partition 1
 271   summary = "mean",   #sets summary stats to get from summary tree nodes
 272   branch_size = 1.5, tip_size = 3,           #sets size for tree elements
 273   xlim = c(-450, -260), nbreaks = 8, geo_size = list(3, 3), #sets geoscale
 274   threshold = c("1 SD", "3 SD"))           #sets selection threshold
 275
 276 #Repeat previous step for clock partitions 2 and 3 (objects S2 and S3)
 277
 278 S1|S2|S3
  
```



273 **Fig. 4.** Relative rates of evolution and inferred mode of selection across morphological
 274 partitions. Scale bars indicates evolutionary rate thresholds for inferring selection mode: 1
 275 standard deviation (weak) and 3 standard deviation (very strong) evidence for positive (red
 276 spectrum) or stabilizing (blue spectrum) modes of selection at each branch for every
 277 morphological partition.

280 Summary statistics of evolutionary rates for each designated clade or clock partition can
281 be extracted from the rates tables and summarized and plotted using the functions
282 *clockrate_summary* and *clockrate_dens_plot*, respectively (Fig. 3). Linear regression models
283 between clock rates are available through the *clockrate_reg_plot* function (Fig. 3), enabling the
284 user to verify the degree of correlation between separate clock partitions. These correlations can
285 be used as the basis to test, for instance, correlated evolution among separate morphological
286 partitions and thus act as a test for evolutionary integration among such partitions (Simões et al.,
287 2020). For plotting individual clock rates and their variance throughout branches in summary
288 evolutionary trees, we suggest several functions available in the package *ggtree* (Yu et al., 2017).

289 In order to infer selection mode, users must obtain posterior estimates for the base of the
290 clock rate value, which are reported in parameter log files from Bayesian inference software.
291 Extracting this parameter from parameter files—and other parameters to be used later for FBD
292 diversification rates (see more below)—requires importing all parameter files and combining them
293 into a single file. This is done with the function *combine_log*, which also allows users to drop
294 samples from generations in the beginning of each log file (i.e., discarded as burn-in) and/or
295 downsampled to reduce the size of the output object (Fig. 4). Hence, *combine_log* is functionally
296 analogous to LogCombiner from the BEAST2 software package (Bouckaert et al., 2019), but
297 specifically targeted to parameter files produced by Mr. Bayes. In practice, users can also use
298 LogCombiner to combine parameter log (.p) files from Mr. Bayes, but we chose to include a
299 standalone function for this purpose to avoid dependency on external software and to conduct all
300 analyses in this pipeline within the R environment.

301 Once rate tables (with customized clade names) and a single parameter file are available, users
302 can deploy the *get_pwt_rates* function, which converts relative rates to absolute rate values and
303 compares rates across every branch and every clock partition to the base of the clock rate
304 (background rate), to measure the degree of rate deviation from background levels (Fig. 4).
305 Thresholds must be defined to establish the degree of rate deviation from background levels that
306 will be used to indicate whether branches and/or morphological partitions are significantly
307 accelerating or decelerating. *EvoPhylo* allows users to utilize flexible thresholds that take into
308 account the dispersion of the distribution of the base rates obtained from the posterior parameter
309 files. For instance, Simões & Pierce (2021) established ± 1 standard deviation (1σ) from the
310 background mean rate as their threshold: a rate of evolution on a given branch greater than the
311 mean background rate +1 standard deviation ($\Delta v > \mu_{\Delta v} + 1\sigma$) indicates an instance of positive
312 selection; a rate of evolution on a branch less than the mean background rate -1 standard
313 deviation ($\Delta v < \mu_{\Delta b} - 1\sigma$) indicates an instance of stabilizing selection or stasis; and a rate of
314 evolution on a branch within 1 standard deviation of the mean background rate ($\mu_{\Delta b} - 1\sigma <$
315 $\Delta v < \mu_{\Delta b} + 1\sigma$) indicates an evolutionary rate not significantly different from the null
316 hypothesis of neutral evolution.

317 *EvoPhylo* allows users to compute multiple threshold levels across the tree using, e.g., one,
318 two, three, or more standard deviations. Users can plot only one of these thresholds or all of them
319 combined onto the evolutionary tree to assess the degree upon which clades are evolving faster or
320 slower compared to background rates, with direct implications for interpreting the mode of

321 selection operating upon the morphological traits (Fig. 4). Hence, here we suggest the
 322 interpretation of the threshold values as: $\pm 1\sigma$ ($p = 0.32$), $\pm 2\sigma$ ($p = 0.05$), $\pm 3\sigma$ ($p = 0.01$) to
 323 indicate weak, strong, and very strong evidence for deviation from background rates, respectively.
 324 These thresholds can all be supplied to the `plot_treerates_sgn` function, which plots the summary
 325 Bayesian evolutionary tree across branches to infer selection mode.
 326

```

### 1. Reshape combined log file from previous steps.
posterior3p_long <- FBD_reshape(Comb_posterior3p)

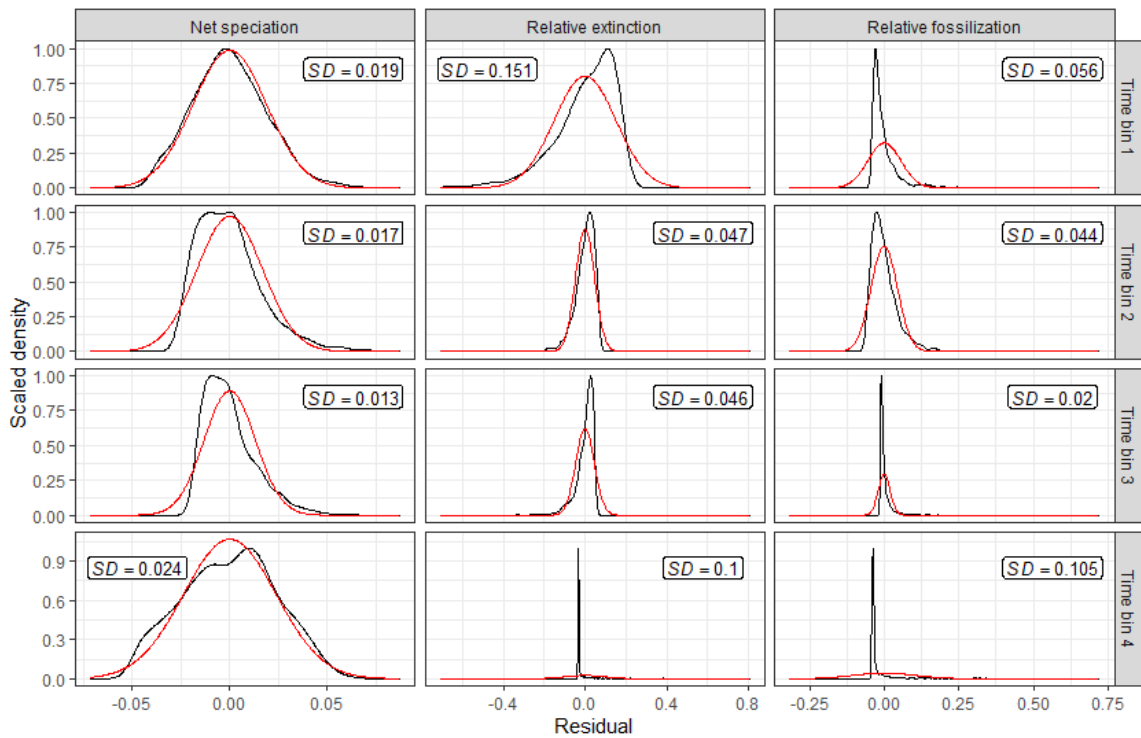
### 2. Summary stats for FBD parameters by time bin
t3.1 <- FBD_summary(posterior3p_long)

### 3. Test for assumptions: normality and homoscedasticity for FBD parameters
# Results = Shapiro-Wilk, Bartlett's and Fligner-Killeen tests
t3.2 <- FBD_tests1(posterior3p_long)

### 4. Visualize deviations from normality and similarity of variances
FBD_normality_plot(posterior3p_long)

### 5. Test for significant FBD shifts between time bins for each FBD parameter
#Results = Pairwise t-tests and Mann-Whitney tests
t3.3 <- FBD_tests2(posterior3p_long)

```



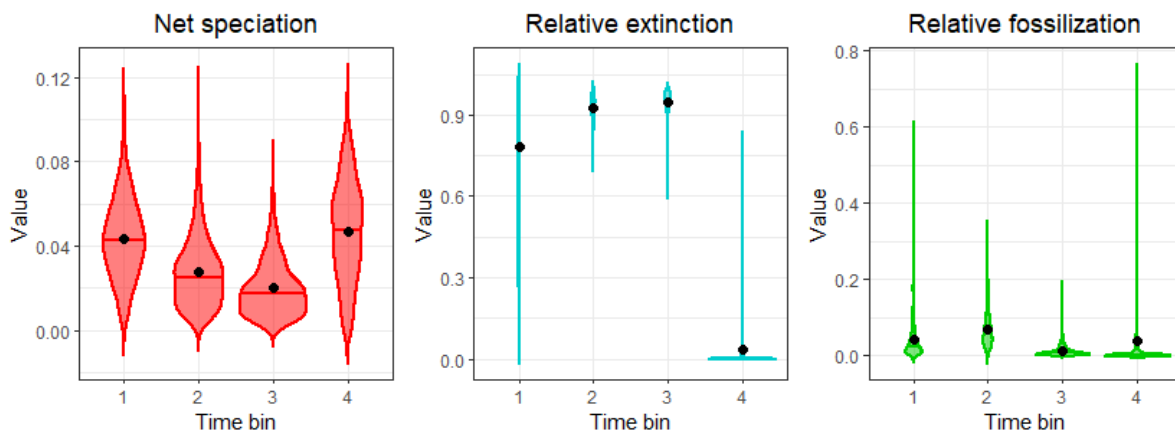
327
 328 **Fig. 5.** Visualization of deviations from normality for each diversification parameter in the FBD
 329 model for every time bin.
 330

331 4. DIVERSIFICATION RATES

332 The skyline variation of the fossilized birth-death tree model (SFBD) (Zhang et al., 2016) has
 333 made it possible to answer some of the most fundamental questions in macroevolution within an
 334 integrated Bayesian evolutionary inference framework and involves estimating net diversification,
 335 relative extinction (turnover), and relative fossilization across time bins. It relaxes the assumption
 336 of previous versions of the FBD model in which all diversification parameters are assumed to be
 337 constant across the tree, which is unrealistic for deep time studies. As with the birth-death skyline
 338 model (Stadler, 2011), the process starts at the root/origin (t_0 or t_{mtca}) and has a number (l) of
 339 rate shifting times (t_i) [t_i ($i = 1, \dots, l$)]. The cutoff time x_{cut} represents the time after which no
 340 more fossils are sampled, and all lineages lead to extant taxa. FBD parameters must be constant
 341 within each time interval $t_i - t_{i-1}$ (or time bins), but they are allowed to vary across them. In its
 342 current implementation, the specific rate shift time points must be prespecified by the user. The
 343 output of SFBD analyses includes posterior estimates for each FBD parameter for every time bin,
 344 thus revealing fundamental aspects of shift in organismal diversity rates across time.
 345

```

  346 ### 5. Plot the distribution of each FBD parameter by time bin with a violin plot
  347 p1 <- FBD_dens_plot(posterior3p_long, parameter = "net_speciation",
  348                   type = "violin", stack = FALSE, color = "red")
  349 p2 <- FBD_dens_plot(posterior3p_long, parameter = "relative_extinction",
  350                   type = "violin", stack = FALSE, color = "cyan3")
  351 p3 <- FBD_dens_plot(posterior3p_long, parameter = "relative_fossilization",
  352                   type = "violin", stack = FALSE, color = "green3")
  353 library(patchwork)
  354 p1 + p2 + p3 + plot_layout(nrow = 1)
  
```



346
 347 **Fig. 6.** Visualization of posterior estimates for each diversification parameter in the FBD model
 348 for every time bin.
 349

350 *EvoPhylo* includes specific functions to combine and assess posterior parameters estimates
 351 from parameter log files (*combine_log*, as described above), including FBD parameters. Using the
 352 *FBD_summary* function to assess the combined parameter log file, users can produce a summary
 353 table of each specific FBD parameter for every time bin. Subsequently, users can use *FBD_tests1*
 354 to assess the normality of the distribution for each FBD parameter in each time bin using the
 355 Shapiro-Wilk normality test and visual assessment of data distribution using *FBD_normality_plot*

356 (Fig. 5). Additionally, *FBD_tests1* also runs a Bartlett and Fligner-Killeen tests of homogeneity of
357 variances to assess homoscedasticity in the data. Finally, for testing between significant parameter
358 rate shifts across time bins, *EvoPhylo* provides fast outputs of parametric (pairwise t-tests) and
359 nonparametric (pairwise Wilcoxon rank sum, or Mann-Whitney) tests through the function
360 *FBD_tests2*. To observe the final distribution of FBD parameters across each time bin, users can
361 deploy *FBD_dens_plot* for each parameter of interest, using different plotting styles passed
362 through *ggplot2* (Wickham, 2016) (Fig. 6).

363 5. CONCLUSIONS

364 Relaxed clock Bayesian evolutionary inference (BEI) is a powerful multivariate statistical
365 approach which enables jointly estimating tree topology and macroevolutionary parameters, such
366 as divergence times, evolutionary rates, and rates of lineage diversification. Several advances in
367 the past decade have made BEI increasingly feasible computationally and parameter rich by the
368 incorporation of a vast array of new trees and clock models. As a result, BEI has been increasingly
369 adopted by evolutionary biologists working with molecular, morphological, and combined datasets
370 to estimate time-calibrated trees and macroevolutionary dynamics across the tree of life. However,
371 the development of bioinformatics tools to preprocess morphological data and postprocess
372 evolutionary parameter estimates from BEI have been somewhat limited.

373 Here we introduce *EvoPhylo*, an R package to extract, plot, statistically summarize, and
374 conduct further downstream analyses from evolutionary parameters obtained from relaxed clock
375 BEI. This includes: automatically detecting partitions in morphological datasets, creating plots and
376 summary statistics for clade and partition specific rates of morphological evolution, inferring
377 significant shifts in evolutionary rates to infer the mode of selection across lineages and
378 morphological partitions, and creating plots and statistically testing for shift in diversification
379 parameters of the fossilized birth death model (net diversification, relative extinction, and relative
380 fossilization) across time. The first version of *EvoPhylo* (v. 0.1) is designed to work with input and
381 output data from the widely used software Mr. Bayes (Ronquist et al., 2012), but an upcoming
382 release will expand its functionalities to also work with output data from the BEAST2 (Bouckaert
383 et al., 2019) software package. *EvoPhylo* will thus facilitate macroevolutionary analyses using
384 Bayesian relaxed clocks for a wide range of users and fields of research, especially those that use
385 morphological datasets.

386

387 5.1 Dependencies

388 *EvoPhylo* depends on several R packages, in particular, *ape* (Paradis & Schliep, 2019), *cluster*
389 (Maechler et al., 2012), *deeptime* (Gearty, 2021), *ggplot2* (Wickham, 2016), *ggrepel* (Slowikowski
390 et al., 2018), *ggtree* (Yu et al., 2017), *patchwork* (Pedersen, 2019), *treeio* (Wang et al., 2020),
391 *Rtsne* (Krijthe, 2015), and *unglue* (Fabri, 2020).

392

393 **ACKNOWLEDGMENTS**

394 We are thankful to the input provided by the members of the Pierce lab during the conduction of
395 this project, as well as discussions with C. Zhang. We thank the provision of a National Sciences
396 and Engineering Council of Canada (NSERC) Postdoctoral Fellowship to TRS. We thank the
397 provision of an European Union’s Horizon 2020 Research and Innovation Programme under the
398 Marie Skłodowska-Curie grant agreement No. 101022928 to J.B.S. Additional funds were
399 provided by Harvard University to S.E.P.

400

401 **CONFLICTS OF INTEREST**

402 The authors declare no conflicts of interest.

403

404 **AUTHOR’S CONTRIBUTIONS**

405 T.R.S. and S.E.P. conceptualize the project. T.R.S., N.G., and J.B-S contributed with code and
406 examples. T.R.S. drafted the manuscript. All authors contributed with discussions, editing, and
407 approved the final version of the manuscript.

408

409 **PEER REVIEW**

410 The peer review history for this article is available at XXX.

411

412 **DATA AVAILABILITY STATEMENT**

413 *EvoPhylo* is hosted on CRAN (<https://cran.r-project.org/package=evophylo>) and available on
414 GitHub (<https://github.com/tiago-simoes/evophylo>). All example datasets are freely available
415 and come bundled with the R package.

416

417 **ORCID**

418 Tiago R. Simões: <https://orcid.org/0000-0003-4716-649X>

419 Noah Greifer: <https://orcid.org/0000-0003-3067-7154>

420 Joëlle Barido-Sottani: <https://orcid.org/0000-0002-5220-5468>

421 Stephanie E. Pierce: <https://orcid.org/0000-0003-0717-1841>

422

423 **REFERENCES**

- 424 Baker, J., Meade, A., Pagel, M., & Venditti, C. (2016). Positive phenotypic selection inferred from
 425 phylogenies. *Biological Journal of the Linnean Society. Linnean Society of London*,
 426 *118*(1), 95–115.
- 427 Bielejec, F., Lemey, P., Baele, G., Rambaut, A., & Suchard, M. A. (2014). Inferring heterogeneous
 428 evolutionary processes through time: from sequence substitution to phylogeography.
 429 *Systematic Biology*, *63*(4), 493–504.
- 430 Bouckaert, R. R. (2010). DensiTree: making sense of sets of phylogenetic trees. *Bioinformatics* ,
 431 *26*(10), 1372–1373.
- 432 Bouckaert, R., Vaughan, T. G., Barido-Sottani, J., Duchêne, S., Fourment, M., Gavryushkina, A.,
 433 Heled, J., Jones, G., Kühnert, D., De Maio, N., Matschiner, M., Mendes, F. K., Müller, N.
 434 F., Ogilvie, H. A., du Plessis, L., Poppinga, A., Rambaut, A., Rasmussen, D., Siveroni, I.,
 435 ... Drummond, A. J. (2019). BEAST 2.5: An advanced software platform for Bayesian
 436 evolutionary analysis. *PLoS Computational Biology*, *15*(4), e1006650.
- 437 Budiaji, W., & Leisch, F. (2019). Simple K-Medoids Partitioning Algorithm for Mixed Variable
 438 Data. *Algorithms*, *12*(9), 177.
- 439 Drummond, A. J., Ho, S. Y. W., Phillips, M. J., & Rambaut, A. (2006). Relaxed Phylogenetics
 440 and Dating with Confidence. *PLoS Biology*, *4*(5), e88.
- 441 Duchêne, S., Molak, M., & Ho, S. Y. W. (2014). ClockstaR: choosing the number of relaxed-clock
 442 models in molecular phylogenetic analysis. *Bioinformatics* , *30*(7), 1017–1019.
- 443 Fabri, A. (2020). unglue: Extract Matched Substrings Using a Pattern. *R Package Version 0.1.0*.
 444 <https://CRAN.R-project.org/package=unglue>
- 445 Felsenstein, J. (1985). Phylogenies and the Comparative Method. *The American Naturalist*,
 446 *125*(1), 1–15.
- 447 Fourment, M., & Darling, A. E. (2018). Local and relaxed clocks: the best of both worlds. *PeerJ*,
 448 *6*, e5140.
- 449 Gavryushkina, A., Heath, T. A., Ksepka, D. T., Stadler, T., Welch, D., & Drummond, A. J. (2017).
 450 Bayesian Total-Evidence Dating Reveals the Recent Crown Radiation of Penguins.
 451 *Systematic Biology*, *66*(1), 57–73.
- 452 Gavryushkina, A., Welch, D., Stadler, T., & Drummond, A. J. (2014). Bayesian Inference of
 453 Sampled Ancestor Trees for Epidemiology and Fossil Calibration. *PLoS Computational*
 454 *Biology*, *10*(12), e1003919.
- 455 Gearty, W. (2021). deeptime: Plotting Tools for Anyone Working in Deep Time. *R Package*
 456 *Version 0. 0.5*. <https://CRAN.R-project.org/package=deeptime>
- 457 Goswami, A., & Polly, P. D. (2010). The influence of character correlations on phylogenetic
 458 analyses: a case study of the carnivoran cranium. In A. Goswami & A. Friscia (Eds.),
 459 *Carnivoran Evolution: New Views on Phylogeny, Form and Function* (pp. 141–164).
 460 Cambridge University Press.
- 461 Gower, J. C. (1971). A General Coefficient of Similarity and Some of Its Properties. *Biometrics*,
 462 *27*(4), 857–871.

463 Heath, T. A., Huelsenbeck, J. P., & Stadler, T. (2014). The fossilized birth–death process for
464 coherent calibration of divergence-time estimates. *Proceedings of the National Academy
465 of Sciences*, *111*(29), 2957–2966.

466 Ho, S. Y. W., Phillips, M. J., Drummond, A. J., & Cooper, A. (2005). Accuracy of rate estimation
467 using relaxed-clock models with a critical focus on the early metazoan radiation. *Molecular
468 Biology and Evolution*, *22*(5), 1355–1363.

469 Höhna, S., Landis, M. J., Heath, T. A., Boussau, B., Lartillot, N., Moore, B. R., Huelsenbeck, J.
470 P., & Ronquist, F. (2016). RevBayes: Bayesian Phylogenetic Inference Using Graphical
471 Models and an Interactive Model-Specification Language. *Systematic Biology*, *65*(4), 726–
472 736.

473 Keating, J. N., Sansom, R. S., Sutton, M. D., Knight, C. G., & Garwood, R. J. (2020).
474 Morphological Phylogenetics Evaluated Using Novel Evolutionary Simulations.
475 *Systematic Biology*, *69*(5), 897–912.

476 King, B., Qiao, T., Lee, M. S. Y., Zhu, M., & Long, J. A. (2017). Bayesian Morphological Clock
477 Methods Resurrect Placoderm Monophyly and Reveal Rapid Early Evolution in Jawed
478 Vertebrates. *Systematic Biology*, *66*(4), 499–516.

479 Krijthe, J. H. (2015). Rtsne: T-distributed stochastic neighbor embedding using Barnes-Hut
480 implementation. *R Package Version 0. 13*. <https://github.com/jkrijthe/Rtsne>

481 Lanfear, R., Frandsen, P. B., Wright, A. M., Senfeld, T., & Calcott, B. (2016). PartitionFinder 2:
482 New Methods for Selecting Partitioned Models of Evolution for Molecular and
483 Morphological Phylogenetic Analyses. *Molecular Biology and Evolution*, *34*(3), 772–773.

484 Lee, M. S. Y., Cau, A., Naish, D., & Dyke, G. J. (2014). Sustained miniaturization and anatomical
485 innovation in the dinosaurian ancestors of birds. *Science*, *345*(6196), 562–566.

486 Lee, M. S. Y., Soubrier, J., & Edgecombe, G. D. (2013). Rates of phenotypic and genomic
487 evolution during the Cambrian explosion. *Current Biology: CB*, *23*(19), 1889–1895.

488 Lehmann, O. E. R., Ezcurra, M. D., Butler, R. J., & Lloyd, G. T. (2019). Biases with the
489 Generalized Euclidean Distance measure in disparity analyses with high levels of missing
490 data. *Palaeontology*, *62*(5), 837–849.

491 Lloyd, G. T. (2016). Estimating morphological diversity and tempo with discrete character-taxon
492 matrices: implementation, challenges, progress, and future directions. *Biological Journal
493 of the Linnean Society. Linnean Society of London*, *118*(1), 131–151.

494 Luo, A., Duchêne, D. A., Zhang, C., Zhu, C.-D., & Ho, S. Y. W. (2020). A Simulation-Based
495 Evaluation of Tip-Dating Under the Fossilized Birth–Death Process. *Systematic Biology*,
496 *69*(2), 325–344.

497 Maechler, M., Rousseeuw, P., Struyf, A., Hubert, M., Hornik, K., & Others. (2012). Cluster:
498 cluster analysis basics and extensions. *R Package Version 2.1.3*. [https://CRAN.R-
499 project.org/package=cluster](https://CRAN.R-project.org/package=cluster)

500 Miller, M. A., Pfeiffer, W., & Schwartz, T. (2012). The CIPRES science gateway: enabling high-
501 impact science for phylogenetics researchers with limited resources. *Proceedings of the 1st*

502 *Conference of the Extreme Science and Engineering Discovery Environment: Bridging*
503 *from the EXtreme to the Campus and Beyond*, 1–8.

504 Morlon, H. (2014). Phylogenetic approaches for studying diversification. *Ecology Letters*, 17(4),
505 508–525.

506 Paradis, E., & Schliep, K. (2019). ape 5.0: an environment for modern phylogenetics and
507 evolutionary analyses in R. *Bioinformatics*, 35(3), 526–528.

508 Pedersen, T. L. (2019). patchwork: The Composer of Plots. R package version 1.0. 0. *R Package*
509 *Version 1.1.1*. <https://CRAN.R-project.org/package=patchwork>

510 Pennell, M. W., & Harmon, L. J. (2013). An integrative view of phylogenetic comparative
511 methods: connections to population genetics, community ecology, and paleobiology.
512 *Annals of the New York Academy of Sciences*, 1289, 90–105.

513 Rambaut, A. (2018). *FigTree v1.4*. <http://tree.bio.ed.ac.uk/software/figtree/>

514 Rambaut, A., Suchard, M. A., Xie, D., & Drummond, A. J. (2018). *Tracer v1.7*.
515 <http://beast.bio.ed.ac.uk/Tracer>

516 Rencher, A. C., & Christensen, W. F. (2012). *Methods of Multivariate Analysis* (Vol. 758). John
517 Wiley & Sons.

518 Revell, L. J., Mahler, D. L., Peres-Neto, P. R., & Redelings, B. D. (2012). A new phylogenetic
519 method for identifying exceptional phenotypic diversification. *Evolution; International*
520 *Journal of Organic Evolution*, 66(1), 135–146.

521 Ronquist, F., Huelsenbeck, J., Teslenko, M., & Nylander, J. A. A. (2019). *MrBayes version 3.2*
522 *manual: tutorials and model summaries*.
523 <https://nbisweden.github.io/MrBayes/manual.html>

524 Ronquist, F., Teslenko, M., van der Mark, P., Ayres, D. L., Darling, A., Höhna, S., Larget, B., Liu,
525 L., Suchard, M. A., & Huelsenbeck, J. P. (2012). MrBayes 3.2: efficient Bayesian
526 phylogenetic inference and model choice across a large model space. *Systematic Biology*,
527 61(3), 539–542.

528 Rousseeuw, P. J. (1987). Silhouettes: A graphical aid to the interpretation and validation of cluster
529 analysis. *Journal of Computational and Applied Mathematics*, 20, 53–65.

530 Simões, T. R., Caldwell, M. W., & Pierce, S. E. (2020). Sphenodontian phylogeny and the impact
531 of model choice in Bayesian morphological clock estimates of divergence times and
532 evolutionary rates. *BMC Biology*, 18, 191.

533 Simões, T. R., & Pierce, S. E. (2021). Sustained High Rates of Morphological Evolution During
534 the Rise of Tetrapods. *Nature Ecology & Evolution*, 5, 1403–1414.

535 Simões, T. R., Vernygora, O. V., Caldwell, M. W., & Pierce, S. E. (2020). Megaevolutionary
536 dynamics and the timing of evolutionary innovation in reptiles. *Nature Communications*,
537 11, 3322.

538 Slater, G. J., & Harmon, L. J. (2013). Unifying fossils and phylogenies for comparative analyses
539 of diversification and trait evolution. *Methods in Ecology and Evolution / British*
540 *Ecological Society*, 4(8), 699–702.

541 Slowikowski, K., Schep, A., Hughes, S., Lukauskas, S., Irisson, J.-O., Kamvar, Z. N., Ryan, T.,
542 Christophe, D., Hiroaki, Y., Gramme, P., & Others. (2018). ggrepel: Automatically
543 Position Non-Overlapping Text Labels with “ggplot2.” *R Package Version 0.9.1.*
544 <https://CRAN.R-project.org/package=ggrepel>

545 Stadler, T. (2010). Sampling-through-time in birth–death trees. *Journal of Theoretical Biology*,
546 267(3), 396–404.

547 Stadler, T. (2011). Mammalian phylogeny reveals recent diversification rate shifts. *Proceedings*
548 *of the National Academy of Sciences of the United States of America*, 108(15), 6187–6192.

549 Tribble, C. M., Freyman, W. A., Landis, M. J., Lim, J. Y., Barido-Sottani, J., Kopperud, B. T.,
550 Höhna, S., & May, M. R. (2022). RevGadgets: An R package for visualizing Bayesian
551 phylogenetic analyses from RevBayes. *Methods in Ecology and Evolution / British*
552 *Ecological Society*, 13(2), 314–323.

553 Van Der Maaten, L. (2009). *Learning a parametric embedding by preserving local structure.*

554 Van Der Maaten, L., & Hinton, G. (2008). Visualizing data using t-SNE. *Journal of Machine*
555 *Learning Research: JMLR*, 9(Nov), 2579–2605.

556 Venditti, C., Meade, A., & Pagel, M. (2011). Multiple routes to mammalian diversity. *Nature*,
557 479(7373), 393–396.

558 Vernygora, O. V., Simões, T. R., & Campbell, E. O. (2020). Evaluating the Performance of
559 Probabilistic Algorithms for Phylogenetic Analysis of Big Morphological Datasets: A
560 Simulation Study. *Systematic Biology*, 69(6), 1088–1105.

561 Wang, L.-G., Lam, T. T.-Y., Xu, S., Dai, Z., Zhou, L., Feng, T., Guo, P., Dunn, C. W., Jones, B.
562 R., Bradley, T., Zhu, H., Guan, Y., Jiang, Y., & Yu, G. (2020). Treeio: An R Package for
563 Phylogenetic Tree Input and Output with Richly Annotated and Associated Data.
564 *Molecular Biology and Evolution*, 37(2), 599–603.

565 Warnock, R. C. M., Heath, T. A., & Stadler, T. (2020). Assessing the impact of incomplete species
566 sampling on estimates of speciation and extinction rates. *Paleobiology*, 46(2), 137–157.

567 Warren, D. L., Geneva, A. J., & Lanfear, R. (2017). RWTY (R We There Yet): An R Package for
568 Examining Convergence of Bayesian Phylogenetic Analyses. *Molecular Biology and*
569 *Evolution*, 34(4), 1016–1020.

570 Wickham, H. (2016). *ggplot2: Elegant Graphics for Data Analysis.* Springer-Verlag.

571 Wright, A. M., & Hillis, D. M. (2014). Bayesian Analysis Using a Simple Likelihood Model
572 Outperforms Parsimony for Estimation of Phylogeny from Discrete Morphological Data.
573 *PloS One*, 9(10), e109210.

574 Wright, A., Wagner, P., & Wright, D. (2020). *Testing character-evolution models in phylogenetic*
575 *paleobiology: a case study with Cambrian echinoderms.*
576 <https://doi.org/10.32942/osf.io/ykzg5>

577 Yang, Z. (2014). *Molecular evolution: a statistical approach.* Oxford University Press.

578 Yu, G., Smith, D. K., Zhu, H., Guan, Y., & Lam, T. T.-Y. (2017). Ggtree : An r package for
579 visualization and annotation of phylogenetic trees with their covariates and other associated
580 data. *Methods in Ecology and Evolution / British Ecological Society*, 8(1), 28–36.

- 581 Zhang, C. (2021). Selecting and averaging relaxed clock models in Bayesian tip dating of
582 Mesozoic birds. *Paleobiology*, 1–13.
- 583 Zhang, C., Stadler, T., Klopstein, S., Heath, T. A., & Ronquist, F. (2016). Total-Evidence Dating
584 under the Fossilized Birth–Death Process. *Systematic Biology*, 65(2), 228–249.
585